# Reciprocal interactions between CA1 pyramidal and axo-axonic cells control sharp wave-ripple events

Earl T. Gilbert[1†], Lianne M.F. Klaver[1†], Kaiser C. Arndt[1], Jongwoon Kim[2], Xiaoting Jia[2,3], Sam McKenzie [4*], Daniel Fine English[1*]

**Affiliations**

1. School of Neuroscience, Virginia Tech, Blacksburg, VA;

2. The Bradley Department of Electrical and Computer Engineering, Virginia Tech, Blacksburg, VA;

3. Department of Materials Science and Engineering, Virginia Tech, Blacksburg, VA;

4. Dept. of Neurosciences, University of New Mexico Health Sciences, Albuquerque, NM;.

[†]These authors contributed equally to this work.

* Correspondence to neurodan83@vt.edu and samckenzie@salud.unm.edu

## Summary

Excitation and inhibition compete to organize spike timing of pyramidal cells (PYR) in CA1 during network events, including sharp wave-ripples (SPW-R). Specific cellular-synaptic sources of inhibition in SPW-R remain unclear, as there are >60 types of GABAergic interneurons in CA1. Axo-axonic cells (AAC) are defined by their synaptic targeting of the axon initial segment of

pyramidal cells, potently controlling spike output. The impact of AAC activity on SPW-R is controversial, due mainly to ambiguity of AAC identification. Here we monitored and manipulated opto-tagged AACs in behaving mice using silicon probe recordings. We found a large variability of AAC neurons, varying from enhanced to suppressed spiking during SPW-Rs, in contrast to the near-uniform excitation of other parvalbumin-expressing interneurons. AACs received convergent monosynaptic inputs from local pyramidal cell assemblies, which strongly influenced their participation in SPW-Rs. Optogenetic silencing of AACs increased power and duration of SPW-Rs, recruiting a greater number of PYR, suggesting AACs control SPW-R dynamics. We hypothesize that lateral inhibition by reciprocal PYR-AAC interactions thus supports the organization of cell assemblies in SPW-R.

## Introduction

Inhibitory actions in the cortex and hippocampus are diverse, with >types of inhibitory interneurons existing along a spectrum, with varied genetic profiles, axonal targeting, and state dependent activity[1–5]. Given the complexity that emerges from the nonlinear dynamics of inhibitory interactions among these types, numerous functions have been attributed to both their global and specific operations[6–8]. Studying unique interneuron subtypes in the hippocampus has proven fundamental in understanding mechanisms underlying circuit function, including their role in various network oscillations, learning, place field tuning and replay of experience[3,4,9–13].

Axo-axonic cells (AACs) are anatomically distinct from other interneurons in two ways. First, only AACs target the axon initial segment of principal cells. Second, they do not target other interneuron types or each other, but instead, mutually interact with principal cells[14–16]. Despite the hypothesized importance of their distinct anatomical features, knowledge about AAC firing patterns in the behaving animal and their role in circuit control is limited[3,14,17,18]. Spiking activity of AACs has been mainly examined in connection with hippocampal sharp wave ripples (SPW-R), a network event critical in memory selection and consolidation, but their specific role has remained controversial[3,17–20].

Leveraging the recent availability of the Unc-5b-Cre mouse-line[14], which enables genetic access to AACs, we conducted *in vivo* silicon probe recordings to characterize the spiking activity of CA1 AACs in SPW-R. We report that participation of AACs in SPW-Rs falls along a continuum, driven by diverse interactions with CA1 pyramidal cells. Using optogenetic inhibition of AACs we found that AACs exhibit control over CA1 circuitry during SPW-R. SPW-R that occurred during AAC-OFF epochs were of longer duration and higher power, though unchanged

53 in frequency. Similarly, during AAC-OFF SPW-R, CA1 pyramidal cell recruitment was enhanced,
54 suggesting that the magnitude of circuit activation during SPW-R, and potentially cell assembly
55 selection, is controlled by AACs. These results demonstrate a critical role for AACs in CA1 SPW-
56 R.

57 **Results**

58 To characterize the activity of AACs, we recorded LFP and ensemble spiking in the hippocampal
59 CA1 region of awake mice expressing excitatory or inhibitory opsins in AACs (**Fig 1A**). Selective
60 opsin expression was achieved by injecting AAV2/5 encoding Cre-dependent opsins into the CA1
61 layer of adult Unc5B-CreER mice[14], allowing us to opto-tag AACs. AACs were identified by
62 activation (square pulses of ChR2-expressing AACs; 100ms, 470nm) or inactivation (Arch-
63 expressing AACs; 300ms, 520nm) (**Fig 1B**). We identified cellular-synaptic properties of 42
64 AACs and examined how their reciprocal interactions with CA1 pyramidal cells organize circuit
65 activity during SPW-R.

66

67 **Characteristics of CA1 axo-axonic cells**

68 We quantified physiological metrics of AACs (n=42 AACs, n=9 animals, 19 sessions). The
69 somata of AACs were observed mostly in or close to the pyramidal layer (**Fig 1C,** μ=6.0μm
70 relative to center of pyramidal layer, σ= 215.6) in agreement with previous studies[14,17,19]. Spike
71 width was variable (**Fig 1D**) with a range of 0.18-0.68ms (**Fig 1F,** μ=0.34ms, σ=0.14), as were
72 spike autocorrelations (**Fig 1E**). Mean firing rates were observed from 0.18-32.47hz (**Fig 1G,**
73 μ=11.33hz, σ=8.64), with inter-spike intervals (ISI) ranging between 0.41ms to 285.71ms (**Fig**
74 **1H,** μ=46.39ms, σ=56.29). A small group of AACs showed transiently fast spiking ("bursting")

with a range of 0.0036-0.6621 (burst index is fraction of spikes with less than 6-ms ISI[21]; **Fig 1I,** μ=0.1787, σ= 0.1910). Despite AACs belonging to a single cell-type (as defined by their synaptic targeting), their physiology variable.

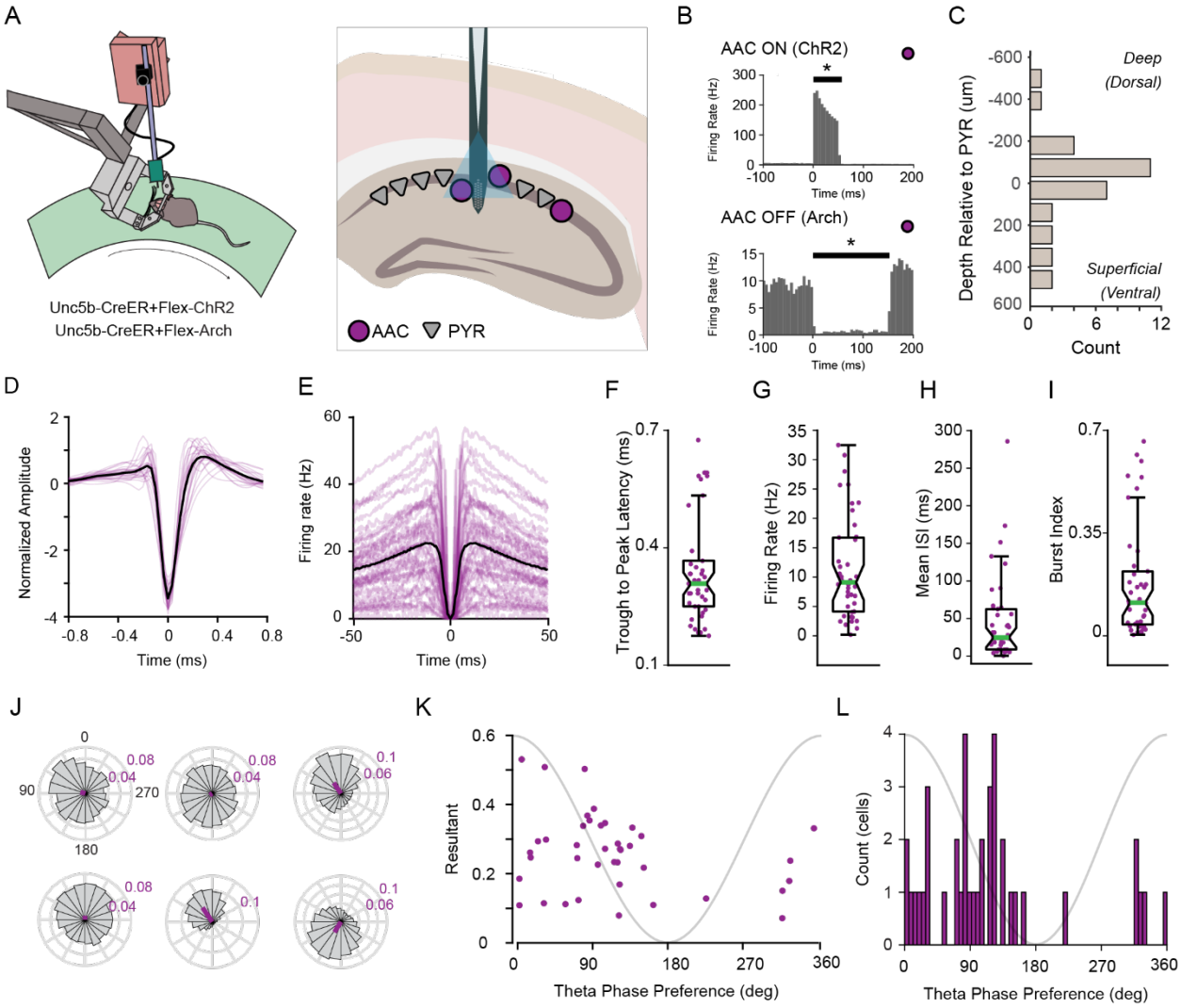


**Figure 1: Firing characteristics of axo-axonic cells**

A.) Cartoon of experimental set-up. Head-fixed mice run on a disc with an acutely implanted silicon probe in CA1 of the hippocampus. A sharpened optic fiber, glued to the probe, is used to stimulate axo-axonic cells.

B.) Example peri-stimulus time histograms of two units' responses to ChR2 (top) or Arch (bottom) activation. Putative interneurons with significant responses to the stimulus were identified as opto-tagged AACs.

C.) Soma position of AACs relative to the pyramidal layer of CA1 (n=32 cells, μ=6.0μm, σ= 215.6)

D.) Average (black) and individual (purple) mean extracellular spike waveforms (n=42 cells)

E.) Average (black) and individual (purple) spike autocorrelations (n=42 cells)

F.) Trough to peak latency of extracellular waveforms. (n=42 cells, $\mu$=0.34, $\sigma$=0.14)

G.) Average firing rate (Hz) of AACs (n=42 cells, $\mu$=11.33Hz, $\sigma$=8.64)

H.) AAC inter-spike-interval (ms, n=42 cells, $\mu$=46.39ms, $\sigma$=56.29)

I.) Distribution of burstiness index (n=42 cells, $\mu$=0.1787, $\sigma$= 0.1910)

J.) Example polar plots of spike entrainment to the theta oscillation of 6 AACs from one recording session.

K.) Theta phase modulation against phase preference of significantly theta modulated AACs (n=40 cells, Circular-linear correlation, rho=0.4147, p=0.0307)

L.) Distribution of significantly theta modulated AACs phase preferences (n=40 cells)

**Axo-axonic cells preferentially spike at the descending phase of the local theta oscillation**

Prior reports have shown strong modulation of AAC spiking by phase of the ongoing theta rhythm[3,17]. Here we report in the largest to date collection of AACs (n=42). We found that many AACs were strongly theta modulated, similar to many CA1 interneurons. Theta phase preference of six AACs from a single recording session are shown in **Fig 1J**, demonstrating the observed variability is not due to inter-animal differences. The majority of AACs exhibit significant theta phase modulation (40/42, **Supplementary Table 1,** Rayleigh z test). Theta phase preference and phase modulation were correlated (**Fig 1K,** rho=.4174, p=0.0307, Circular-linear correlation coefficient), with most cells spiking on the descending phase (**Fig 1L**). The average theta phase preference for the population was 76.34°, while the most theta modulated AAC exhibited a phase preference of 6.45°. AACs as a population are highly theta modulated cells, with a phase preference for the descending phase of the oscillation.

**Axo-axonic cells are activated in SPW-R**

The participation of AACs in CA1 SPW-R is critical to understanding their role in the CA1 circuit, though there are mixed reports as to their level of participation[3,14,17–20]. Ripple-associated spiking activity of 42 AACs (**Fig 2A,** n=42 cells, n=595-16,058, μ=5,666.4 SPW-R per recording session,), revealed diverse participation across the population. On average AACs have significantly increased firing rate during SPW-R (**Fig 2B**, Left: n=42 cells, baseline $\tilde{x}$=6.19hz, SPW-R $\tilde{x}$=11.3hz, p=3.0939e-4, Wilcoxon signed rank test). Interestingly, out of the 39 AACs that changed their firing rate (ZETA[22]) 27 cells increased and 12 cells decreased their activity (**Fig 2B**, Right), which stands in contrast to other interneurons with a more uniform response, such as PV+ cells (**Fig S1,** 43/46 cells showed increased activity). AAC activity was strongly modulated by the phase of individual ripple waves with most cells firing on the ascending phase of the ripple oscillation (100-250Hz, **Fig 2C, $\theta_\mu$**=257.37 degrees).

Single cell ripple modulation values (SPW-R firing rate gain) ranged from .61-3.01 (**Fig 2D,** μ=1.24, σ= 0.45). Average number of spikes in SPW-R ranged from 1.02-4.73 (**Fig 2E**, μ=2.03, σ= 1.02), while inter-spike intervals of AACs in SPW-R ranged from 9.1-37.2ms (**Fig 2F**, μ=19.9ms, σ= 6.7). Additionally, because SPW-R information content systematically varies from the beginning to end of each event, we calculated the average time of the first spike from the peak of the SPW-R, which ranged from -21.7-42.0ms (**Fig 2G**, n=42 cells, μ=-7.7ms, σ=0.0064), suggesting AACs likely influence activity throughout the SPW-R event. Together, these results demonstrate diverse spike responses of AACs in SPW-R, with a majority of AACs significantly increasing firing. These data demonstrate that AACs participate in SPW-R events in behaving mice.

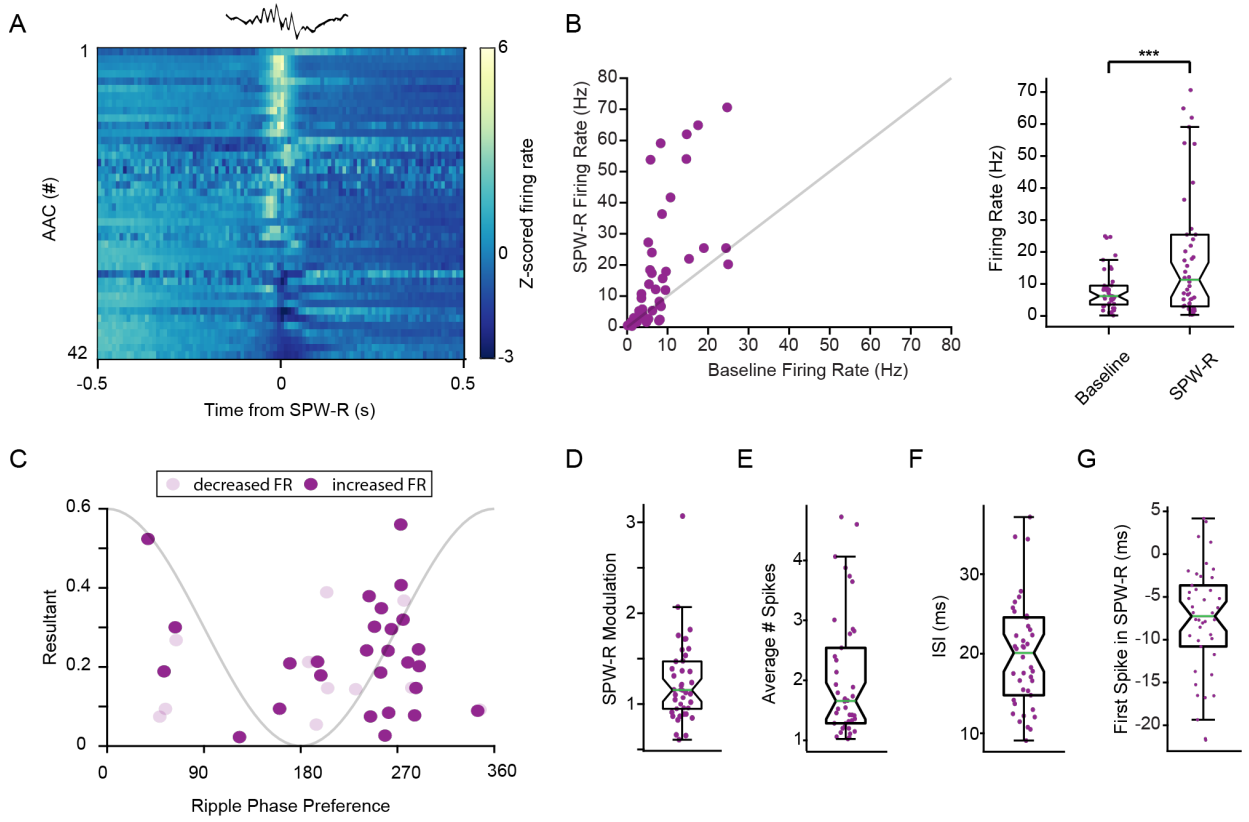


**Figure 2: AACs firing is modulated by sharp wave-ripples**

A.) Peri-event time histogram of AAC z-scored firing rate centered on SPW-R peak (n=42 cells, 1495-16,058 SPW-R events, μ=5,666.4 events)

B.) Left: Scatter plot of baseline firing rate against firing rate during SPW-R of each AAC. (n=42). Right: Firing rate (Hz) in baseline and within SPW-R. (n=42 cells, baseline x̃=6.19Hz, SPW-R x̃=11.3Hz, p=3.0939e-4, Wilcoxon signed rank test)

C.) Ripple wave phase modulation against phase preference of significantly SPW-R modulated AACs (n=39 cells)

D.) Ripple wave phase- modulation of AACs (n=42 cells, μ=1.24, σ= 0.45)

E.) Average number of spikes fired in SPW-R events (n=42 cells, μ=2.03, σ= 1.02)

F.) Inter-spike-interval during SPW-R (n=42 cells, μ=19.9ms, σ= 6.7)

G.) Average delay to first spike in SPW-R from the peak of SPW-R (n=42 cells, μ=-7.7ms, σ=0.0064)

## CA1 pyramidal neurons control the participation of axo-axonic cells in SPW-R

To determine if local excitation is a mechanism by which AAC activity is modulated in SPW-R, we quantified excitatory synaptic inputs from local CA1 PYR. Such monosynaptic

145 connections were identified using a validated monosynaptic inference method[23,24] (based on cross-
146 correlations of putatively-classified pyramidal cells and AACs). For AACs with at least one
147 presynaptic PYR, we calculated the average SPW-R modulation of all presynaptic inputs. Example
148 SPW-R cross-correlations (**Fig 3A**) illustrate both strongly and weakly modulated AACs and their
149 partners (note that an AAC with a large peak in the cross-correlation at the time of SPW-R has
150 partners that also show a large peak, **Fig 3A, top**). AAC ripple modulation correlated with that of
151 its inputs, such that AACs that received synaptic drive from ripple modulated PYR were
152 themselves strongly ripple modulated. (**Fig 3B,** r=0.7453, p=1.9134e-5, Spearman's Rank
153 Correlation; correlation with randomly selected non-presynaptic partner control, r=0.1915
154 p=0.3574, Spearman's Rank Correlation). We found further evidence that the CA1 PYR modulate
155 AAC activity in SPW-R when examining other metrics. We quantified the correlation between
156 spiking activity and power in the ripple frequency band as well as the magnitude of phase
157 modulation. There was a significant relationship between spike rate power correlation of
158 presynaptic PYR and AACs (**Fig 3C**, r=0.4569, p=0.0227, Spearman's Rank Correlation), as well
159 as ripple phase modulation between paired cells (**Fig 3F**, r=0.4092, p=0.0433, Spearman's Rank
160 Correlation). Given the relationship between presynaptic and AAC activity, we investigated the
161 relationship between strength of presynaptic connections and AAC participation in SPW-R. Both
162 AAC SPW-R modulation and time to first spike were related to spike transmission probability.
163 Stronger spike transmission probability was associated with higher ripple modulation (**Fig 3E,**
164 r=0.5354, p=0.0065, Spearman's Rank Correlation), and a shorter delay between first spike and
165 SPW-R peak (**Fig 3F,** r=-0.7108, p=1.0477e-04, Spearman's Rank Correlation). Interestingly, we
166 found a relationship between AAC SPW-R modulation and both soma depth (**Fig S2,** r=-0.3260,
167 p=0.0418, Spearman's Rank Correlation; as has been previously reported[17]) and trough to peak

latency of spikes (**Fig S2,** r=-0.3260, p=0.0429, Spearman's Rank Correlation). No relationship was found between AAC SPW-R modulation and AAC burst index, ISI, or baseline firing rate (**Fig S2,** p>0.05, Spearman's Rank Correlation). Notably, the correlation of soma depth and trough to peak latency to ripple modulation was weaker than any presynaptic-AAC relationships. These results suggest that excitation from CA1 PYR controls AAC activity during SPW-R.

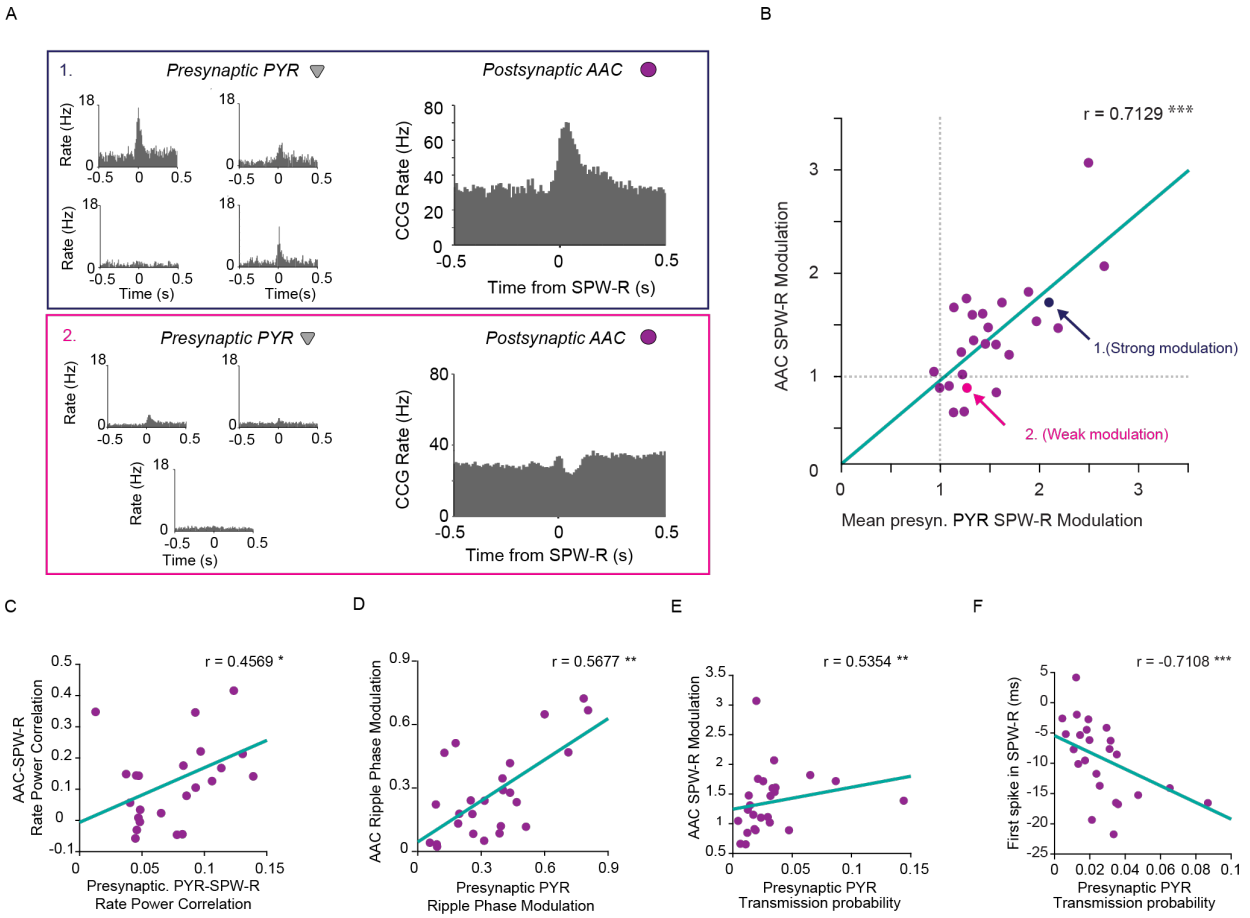


**Figure 3: Local presynaptic pyramidal cells contribute to spiking of AACs in SPW-R**

A.) Top: SPW-R cross-correlograms between 4 pyramidal cells presynaptically (prePYR) connected to a strongly ripple-activated AAC (right). Bottom: Example SPW-R cross-correlograms between 3 pyramidal cells presynaptically connected to a of a weakly ripple modulated AAC.

B.) Correlation between average SPW-R modulation of presynaptic PYR and their monosynaptically connected AACs (n=25 AACs, n=1-8 prePYR, r=0.7453, p=1.9134e-5, Spearman's Rank Correlation). Arrows point to the example sets in A.

C.) Correlation between average rate power correlations of spike to ripple frequency (100-250Hz) power of presynaptic partners and AACs (n=25 AACs, n=1-8 prePYR, r=0.4569, p=0.0227, Spearman's Rank Correlation)

D.) Correlation between average ripple (100-250Hz) phase modulation of presynaptic partners and AACs (n=25 AACs, n=1-8 prePYR, r=0.4092 p=0.0433, Spearman's Rank Correlation)

E.) Correlation between average PYR-AAC spike transmission probability and SPW-R RIPPLE WAVE? modulation of AACs (n=25 AACs, n=1-8 prePYR, r=0.5354, p=0.0065, Spearman's Rank Correlation)

F.) Correlation between average PYR-AAC spike transmission probability and AAC average delay to first spike in SPW-R from peak (n=25 AACs, n=1-8 prePYR, r=-0.7108, p= 1.0477e-04, Spearman's Rank Correlation)

## AACs control network-wide spiking activity and SPW-R dynamics

We found that AACs robustly participate in SPW-R, though whether they influence the generation of SPW-R in the network remains unknown. To address this question, we optogenetically inhibited local AACs expressing archaerhodopsin (Arch). Silencing AACs increased power in the ripple band (100-250hz, **Fig 4A,B**, Bottom: n=5 sessions, 4 mice. n=843-1936 300ms stims. p=0.0020, Paired T-test), as well as power in the 300-500Hz band, which reflects population spiking activity (300-500hz, **Fig 4A,B**, Top: n=5 sessions, 4 mice. n=843-1936 300ms stims. P=3.0224e-04, Paired T-test). We then detected SPW-R and examined properties of such events occurring either in or out of AAC inhibition epochs. When AACs were silenced, ripple band power increased (**Fig 4C**, n=5 sessions, 4 mice. n=1495-12364 control ripples, n= 64-335 stim ripples), as did event durations (**Fig 4E**, n=5 sessions, 4 mice. n=37032 control ripples, n= 1024 stim ripples. p=0.0072, Wilcoxon rank sum-test), and peak amplitude (**Fig 4F**, n=5 sessions, 4 mice. n=37032 control ripples, n=1024 stim ripples. p=2.0593e-06, Wilcoxon rank sum test), while ripple frequency was not affected (**Fig 4D**, n=5 sessions, 4 mice. n=37032 control ripples, n=1024 stim ripples. p=0.8675, Wilcoxon rank-sum test). This suggests that AACs control content and magnitude of SPW-R while other cell types may pace the rhythm (likely basket cells[25]). These data reveal an important role for AACs in controlling SPW-R dynamics at the network level.

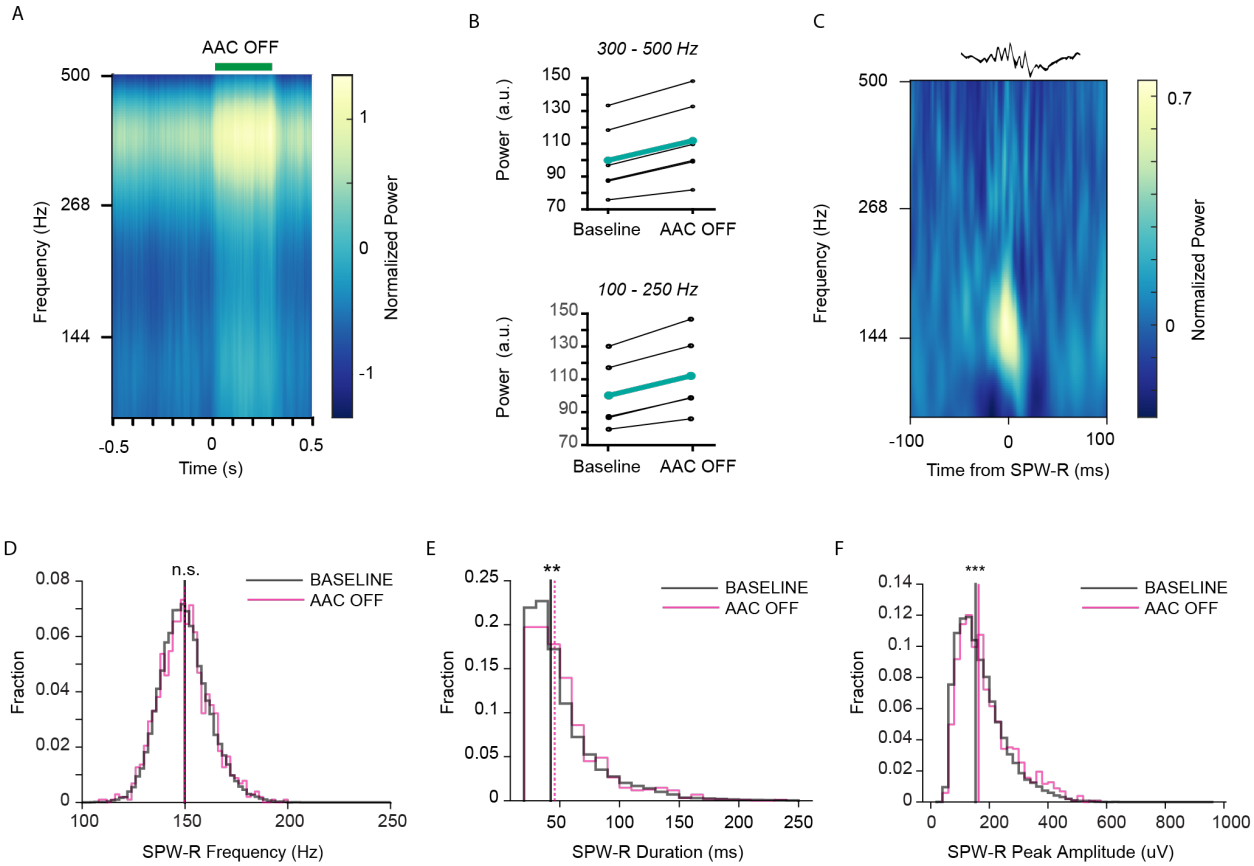


**Figure 4: Axo-axonic cells affect SPW-R dynamics**

A.) Mean peri-stimulus power spectral density (PSD) of AAC-Arch activation (n=5 sessions, 4 mice. n=843-1936 300ms stims)

B.) Average power of PSD in A comparing baseline (-300ms:0ms) to stimulation (0ms:300ms) in the spike band (top, 300-500Hz n=5 sessions, 4 mice. n=843-1936 300ms stims. p=3.0224e-04, Paired T-test) and the SPW-R band (bottom, 100-250Hz. n= 5 sessions, 4 mice. 843-1936 300ms stims. p=0.0020, Paired T-test)

C.) Average SPW-R event PSD of control events subtracted from AAC-OFF events (n=5 sessions, 4 mice. n=1495-12364 control ripples, n=64-335 AAC-OFF ripples.)

D.) Distribution of frequency of AAC-OFF SPW-R events compared to control (n=5 sessions, 4 mice. n=37032 control ripples, n= 1024 AAC-OFF ripples. p=0.8675, Wilcoxon rank sum test.)

E.) Distribution of duration of AAC-OFF SPW-R events compared to control (n=5 sessions, 4 mice. n=37032 control ripples, n= 1024 AAC-OFF ripples. p=0.0072, Wilcoxon rank sum test.)

F.) Distribution of peak amplitude of AAC-OFF SPW-R events compared to control (n=5 sessions, 4 mice. n=37032 control ripples, n= 1024 AAC-OFF ripples. p=2.0593e-06, Wilcoxon rank sum test.)

220 **AACs control pyramidal cell participation in SPW-R**

221 Pyramidal cells are reliably depolarized during SPW-R, and competition between
222 excitatory and inhibitory inputs compete to determine spiking at the single cell level[12]. Given our
223 findings that most AACs are active in SPW-R, and inhibiting them alters SPW-R dynamics, we
224 next investigated the effects of silencing AACs on PYR spiking. We first looked at the effects of
225 manipulating AAC activity in all states. AAC activation inhibited PYR firing, while AAC
226 silencing resulted in PYR disinhibition, revealed by changes in their firing rates. (**Fig 5A**, Left,
227 ChR2: n=11 sessions, 4 mice. n=1063-4459 100ms stims, n=180 PYR, Right, Arch: n=5 sessions,
228 4 mice. n=843-1936 300ms stims, n=207 PYR). These results demonstrate that AACs tonically
229 inhibit PYR. Next, we sought to investigate how AAC inhibition shapes PYR activity selectively
230 during SPW-R by comparing control ripples to ripples that occurred during periods where AACs
231 were silenced. We quantified the fraction of PYR that participated in AAC-OFF SPW-R compared
232 to control. In AAC-OFF SPW-R, we observed a significant increase in PYR participation. (**Fig**
233 **5B**, Left: AAC: n=5 sessions, 4 mice. n=31-55, total: 194 PYR. n=1495-12364, total: 37032
234 Control SPW-R. n=51-287, total: 868 AAC-OFF SPW-R. p=5.2716e-16, Wilcoxon rank-sum
235 test.) Superficial and deep CA1 PYR receive different patterns of inhibition[26,27], thus we quantified
236 this effect separately for each subgroup of pyramidal population. In AAC-OFF SPW-R, the
237 fraction of both superficial and deep PYR participation increased (**Fig S3**, Right: Top, AAC,
238 n=1495-12364, total: 37032 Control SPW-R. n=51-287, total: 868 AAC-OFF SPW-R. n=11-32,
239 total: 125 Deep cells, n=5-33, total: 69 Superficial cells. Deep: p=2.4645e-13, Wilcoxon rank-sum
240 test. Superficial: p=6.5141e-06, Wilcoxon rank-sum test.). Given that cell assemblies constructed
241 from unique sets of PYR enable the encoding of separate experiences by SPW-R[28–31] we examined
242 SPW-R associated PYR activity at an individual cell level. On average, PYR exhibited a higher

count of spikes in AAC-OFF SPW-R (**Fig 5C**, n=5 sessions, 4 mice. n=194 PYR, n=1495-12364 Control SPW-R. n=51-287 AAC-OFF SPW-R. p=6.1155e-08, Wilcoxon signed-rank test). Similarly, pyramidal cell SPW-R firing rate gain was significantly higher when AACs were silenced (**Fig 5D**, n=5 sessions, 4 mice. n=194 PYR, n=1495-12364 Control SPW-R. n=51-287 AAC-OFF SPW-R. p=2.4569e-08, Wilcoxon signed-rank test). Increased firing rate was additionally reflected in decreased inter-spike interval in AAC-OFF SPW-R. (**Fig 5E**, n=5 sessions, 4 mice. n=194 PYR, n=1495-12364 Control SPW-R. n=51-287 AAC-OFF SPW-R. p=6.9834e-05, Wilcoxon signed-rank test.) Further, AACs participated in a higher fraction of total AAC-OFF SPW-R than control SPW-R. (**Fig 5F**, n=5 sessions, 4 mice. n=194 PYR, n=1495-12364 Control SPW-R. n=51-287 AAC-OFF SPW-R. p=1.8104e-11, Wilcoxon signed-rank test). These results demonstrate AACs exert control over PYR spiking in SPW-R.

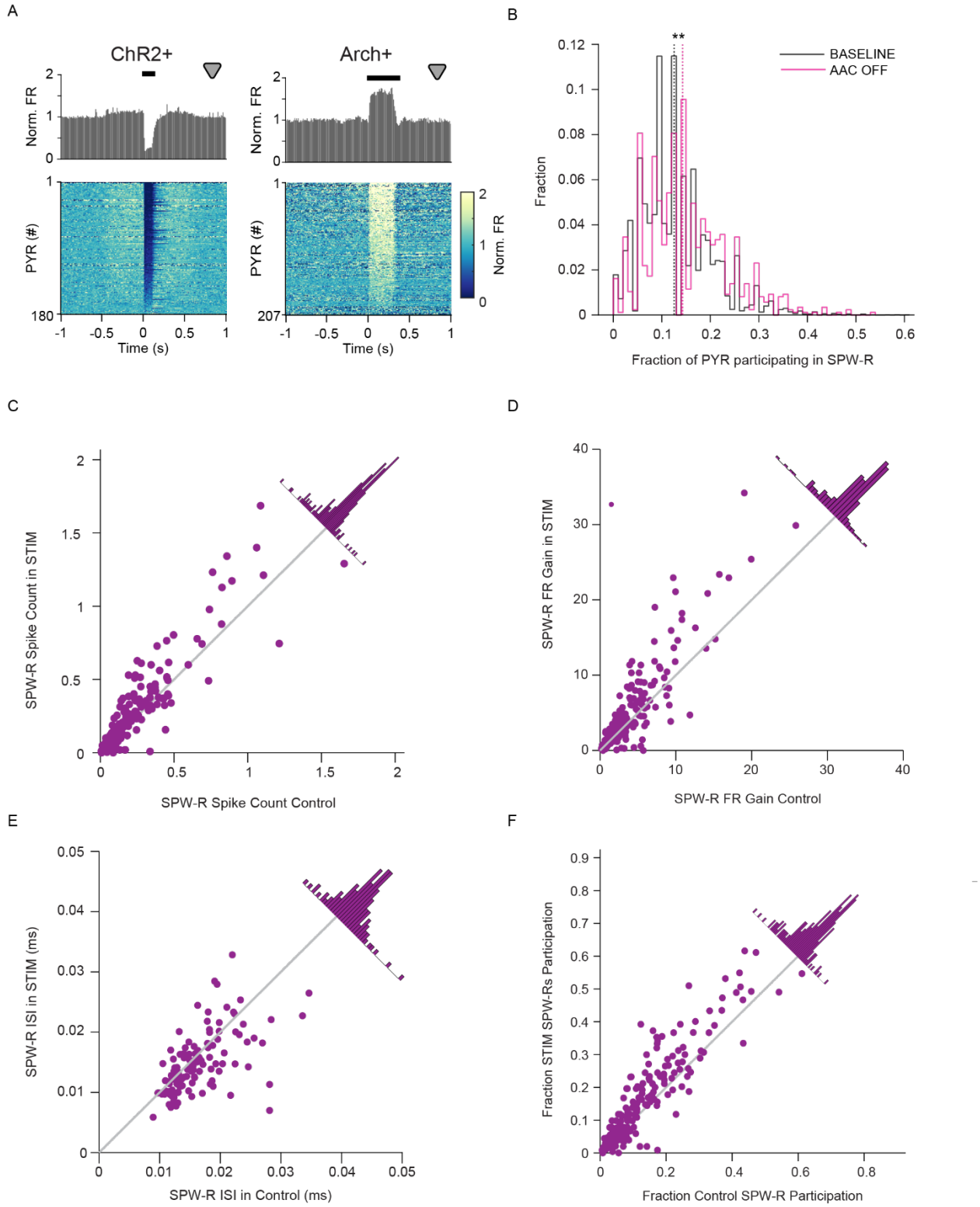


**Figure 5: AACs control pyramidal cell participation during SPW-R**

A.) Peri-stimulus time histograms of PYR firing rate in response to stimulation of interneurons in a subset of sessions with matched stim durations. (**Left**, ChR2: n=11 sessions, 4 mice. n=1063-4459 100ms stims, n=180 PYR, **Right**, Arch: n=5 sessions, 4 mice. n=843-1936 300ms stims, n=207 PYR)

B.) Distribution of fraction of PYR participating in control and AAC-OFF SPW-R. (n=5 sessions, 4 mice. n=31-55, total: 194 PYR. n=1495-12364, total: 37032 Control SPW-R. n=51-287, total: 868 AAC-OFF SPW-R. p=5.2716e-16, Wilcoxon rank-sum test.)

C.) Scatter plot of individual PYR mean spike count in control against count in AAC-OFF SPW-R. Gray: Unity Line. Distribution of distances from unity line on diagonal. (n=5 sessions, 4 mice. n=194 PYR, n=1495-12364 Control SPW-R. n=51-287 AAC-OFF SPW-R. p=6.1155e-08, Wilcoxon signed-rank test)

D.) Scatter plot of individual PYR firing rate gain in control against firing rate gain in AAC-OFF SPW-R. Gray: Unity Line. Distribution of distances from unity line on diagonal. n=5 sessions, 4 mice. n=194 PYR, n=1495-12364 Control SPW-R. n=51-287 AAC-OFF SPW-R. p=2.4569e-08, Wilcoxon signed-rank test)

E.) Scatter plot of individual PYR inter-spike interval in control against inter-spike interval in AAC-OFF SPW-R. Gray: Unity Line. Distribution of distances from unity line on diagonal. (n=5 sessions, 4 mice. n=194 PYR, n=1495-12364 Control SPW-R. n=51-287 AAC-OFF SPW-R. p=6.9834e-05, Wilcoxon signed-rank test.)

F.) Scatter plot of fraction of control SPW-R in which individual PYR participated against participation in AAC-OFF SPW-R. Gray: Unity Line. Distribution of distances from unity line on diagonal. (n=5 sessions, 4 mice. n=194 PYR, n=1495-12364 Control SPW-R. n=51-287 AAC-OFF SPW-R. p=1.8104e-11, Wilcoxon signed-rank test.)

# Discussion

Glutamatergic excitation and GABAergic inhibition compete to control PYR participation in SPW-R[25]. In each SPW-R, only a minority of PYR spike even though Vm is depolarized above spike threshold for 10's of milliseconds, due to dynamically balanced GABAergic inhibition. Inhibition thus plays a critical role in enabling competition-based selection and expression of PYR assemblies. Identifying the source(s) of this inhibition is critical to understanding the CA1 circuit, and likely arises from axo-somatic targeting cells such as basket cells and AACs. Here we identify novel mechanisms by which AACs participate in and control CA1 SPW-R. Notably, reciprocal

interactions between excitatory PYR and inhibitory AACs organize cell assembly and network activity during SPW-R.

**Recruitment of AACs to sharp wave-ripples is explained by monosynaptic inputs from CA1 PYR**

CA1 interneuron spiking is controlled both by afferent inputs (e.g., CA3) and excitation and inhibition from local PYR and INT, respectively[32–34]. To determine the activity of AACs and PYR during SPW-R at single-spike resolution, we used silicon probes to obtain CA1 ensemble recordings and opto-tagged AACs. As a population, AAC activity is significantly increased during SPW-R, with a minority of cells exhibiting decreased activity (**Fig 2A,B)**. In agreement with these findings, up- and down-modulated AACs have been previously described in studies using both juxta-cellular electrophysiology[26] and calcium imaging[14,19]. To better understand the driver of AAC spiking in SPW-R, we examined their somatic location, physiology and excitatory inputs from CA1 PYR. Individual AAC activity in SPW-R is strongly correlated with the activity of presynaptic partners and the strength of these connections (**Fig 3)**. Thus, local excitation drives AAC activity in SPW-R. Importantly, it remains unknown if the propensity for AACs to participate in SPW-R is consistent across experiences and/or throughout the lifespan of the animal[35]. Such plasticity could be supported both by changes in excitatory inputs we identified as well as inhibition from local interneurons[36]. Longitudinal recording of single AACs would be required to answer these questions.

**AACs control network activation and PYR spiking in sharp wave-ripples**

Silencing AACs led to increased power in both the spiking band and SPW-R band (**Fig 4A,B**), SPW-R events that occurred during AAC silencing were of longer duration, and had higher

304 power and peak amplitude (**Fig 4C,F,G**). Interestingly AAC silencing did not alter SPW-R
305 frequency. These data support a model in which AACs robustly control PYR recruitment, while
306 other interneurons or time constants may play a more important role in synchronizing PYR
307 populations at ripple frequency.

308 PYR activity in SPW-R was affected significantly by silencing AACs. Inhibition of AACs
309 increased the number of participating PYR (**Fig 5B)** and produced increased average spike count,
310 firing rate gain and decreased inter-spike intervals of PYR (**Fig 5C,D,E)**. Additionally, PYR
311 participated in a greater fraction of AAC-OFF epochs than during control SPW-R, suggesting a
312 SPW-R-related gain. Our findings that during SPW-R, silencing AACs disinhibits PYR, and that
313 PYR drive AAC spiking, suggests lateral inhibition is instantiated by reciprocal interactions
314 between pyramidal cells and AACs. These results support the general hypothesis that individual
315 interneurons serve unique functions in CA1 circuit computations, and that this mechanism supports
316 the construction of and competition between cell assemblies. Our experiments demonstrate this
317 specifically for the understudied AAC interneuron family.

318 # Methods

319 All protocols and experiments using animals were approved by the Virginia Tech (Blacksburg,
320 VA, USA) Institutional Animal Care and Use Committee (IACUC)

321 **AAV Injection**

322 Mice are induced and maintained at a surgical plane of anesthesia with isoflurane while mounted
323 in a stereotaxic frame. Hair is removed and scalp is disinfected. Bupivicaine is injected once
324 under the scalp before revealing skull. A < 0.2 mm burr hole is made above area CA1 of the
325 hippocampus in both hemispheres. (mm from bregma: −1.8, lateral: +/-1.5). Glass pipette
326 containing AAV5-EF1a-DIO-hChR2 (H134R)-EYFP or AAV5-EF1a-DIO-eArch3.0-EYFP
327 (UNC Gene Therapy Center – Vector Core) is lowered into CA1 using stereotaxic coordinates.
328 100nL of AAV (titer: 3.8-5.2x$10^{12}$ GC/mL) is injected into tissue (1nL$s^{-1}$) using a nanoliter
329 injector (WPI: MICRO2T & 504127). Following infusion, the glass pipette is left to rest for 5
330 minutes before slowly removing from the brain. The scalp is then closed with Vetbond (3M).

331 **Tamoxifen injections**

332 Mice were injected intraperitoneally with tamoxifen (100 mg/kg) dissolved in corn oil at 20
333 mg/ml on days 5,7, and 9 following AAV injection.

334 **Head-bar Implantation**

335 Mice are induced and maintained at a surgical plane of anesthesia with isoflurane while mounted
336 in a stereotaxic mount. Bupivicaine is injected under the scalp before it is removed. The skull is
337 cleaned with 3% hydrogen peroxide, followed by an application of dental adhesive Optibond
338 (Kerr Dental). A small burr hole is made above cerebellum, and a stainless-steel ground wire is

339 inserted between the skull and the brain, parallel to the brain surface, then the wire is affixed to
340 the skull with sterile dental acrylic. A headplate is positioned parallel to the skull above lambda,
341 and is permanently fixed in place.

342 **Craniotomy**

343 One day before recording, mice are induced and maintained at a surgical plane of anesthesia with
344 isoflurane while mounted in the stereotaxic mount. A <1.0 mm burr hole is made above the
345 hippocampus and the dura is removed. Kwik-cast (World Precision Instruments) is applied to the
346 burr hole, with dental acrylic applied on top, to protect the craniotomy until recording.

347 ***In Vivo* recording**

348 Unc5b-CreER mice were obtained from the lab of Z. Josh Huang under full MTA. All animals
349 used in experiments were homozygous Unc5b-CreER or hybrid Unc5b-CreER x FVB/NJ (JAX
350 #001800) mice. Additionally, PV-Cre mice were acquired from the Jackson Laboratory (Jax
351 #017320). During the time of experiments, mice were between the ages of 16–30 weeks old.
352 Mice of both sexes were used in all experiments. Mice, trained and habituated to head-fixed
353 navigation, are placed in the head fixation apparatus, and a silicone probe (Poly3, Neuronexus, or
354 P1, Cambridge Neurotech, with optic fiber attached, or 4x8 uLED, Neurolight technologies), is
355 lowered through the craniotomy into the brain until SPW-R are observed and left in place for 30-
356 45 minutes until tissue is relaxed. The neural signals were amplified, digitized and recorded with
357 RHD2000 system (Intan Technologies LLC).

358 **Optical Stimulation**

359 Optical pulses were delivered through a sharpened optic fiber connected to a Thorlabs laser
360 diode driver and laser diode or optical pulses are delivered through LEDs in a 4x8 uLED probe
361 (Neurolight Technologies).

362 **Data collection**

363 Unc5b-CreER ChR2, Arch, and PV+ data was collected for this study. A selection of PV+ data
364 was used with permission from the Buzsaki Data Repository[24,37].

365 **Data analysis**

366 Data analysis was conducted in Matlab (Mathworks) and custom scripts were used to analyze the
367 extracellular and spike data. Spike sorting was performed using Kilosort1[38] with custom semi-
368 automated reclustering[39] followed by manual curation using Phy. Cell Explorer[40] was used to
369 characterize neuron properties including cell position, autocorrelation, wave form characteristics,
370 firing rate characteristics, putative monosynaptic connections (followed by manual refinement)
371 and SPW-R modulation. The Buzcode repository was used to calculate cross correlations and for
372 SPW-R detection. The HippoCookBook repository and Circular Statistics Toolbox (Mathworks)
373 were used to quantify oscillation phase preference and phase modulation. Rate power correlation
374 was calculated by correlating spike trains with power in the SPW-R band (100-250Hz). Opto-
375 tagged AACs were identified using CellExplorer to classify putative cell type, and Zenith of Event-
376 based Time-locked Anomalies (ZETA[22]) to determine significance of the response to stimulation.
377 Further, opto-tagged AACs were manually refined through observation of peri-stimulation time
378 histogram to optical stimulation. Significance of SPW-R modulation was determined using
379 CellExplorer and ZETA. For detection of SPW-R characteristics in and out of stimulation (Fig 4),
380 SPW-R were classified as having the peak of the event within stimulation times. For detection of

spikes from cells in SPW-R events (Fig 5), only SPW-R that had the entire duration within a stimulation pulse were considered INT-OFF SPW-R.

## Author Contributions

E.G., L.M.F.K., S.M., and D.F.E. designed the study. E.G., S.M., L.M.F.K and D.E. conducted experiments. E.G., L.M.F.K., K.A., J.K., S.M., and D.F.E. conducted data analysis. All authors contributed to the writing of the manuscript.

## Supplemental Information

### Table 1: Quantification of AAC characteristics

| AAC ID | Position | Trough to Peak | AB Ratio | Firing Rate | ISI | Burst Index | Theta Phase Preference | Theta Phase Modulation | Theta, Rayleigh's Z p Value | Baseline Firing Rate | SPW-R Firing Rate | SPW-R ZETA p value | SPW-R Phase Preference | SPW-R Phase Modulation | SPW-R, Rayleigh's Z p Value | SPW-R Modulation | SPW-R Avg # Spikes | SPW-R ISI | SPW-R Time to First Spike | Average Partner SPW-R Modulation | SPW-R Rate Power Correlation | Average Partner SPW-R Rate Power Correlation | Average Partner SPW-R Phase modulation | Average Partner Transmission Probability |
|---|---|---|---|---|---|---|---|---|---|---|---|---|---|---|---|---|---|---|---|---|---|---|---|---|
| 1 6 | -129.7036144 | 0.358333333 | 0.517676112 | 2.45659825 | 4.194044457 | 0.033225337 | 1.867729722 | 0.346354849 | 1.71521E-83 | 1.750663184 | 2.170900445 | 0.001289698 | 4.881621794 | 0.211475012 | 5.20365E-11 | 0.958106638 | 1.058951965 | 0.034704938 | 0.032934473 | NaN | 0.013634235 | NaN | NaN | NaN |
| 1 8 | -4.703614369 | 0.275 | 0.305668564 | 2.446166462 | 8.631051532 | 0.174530493 | 1.726930991 | 0.339490704 | 8.89021E-36 | 1.043222309 | 1.663007355 | 6.33823E-05 | 1.104397112 | 0.30039366 | 1.80137E-16 | 1.158013544 | 1.04735376 | 0.021223529 | 0.033319555 | NaN | 0.029109153 | NaN | NaN | NaN |
| 2 4 | 512.1489619 | 0.533333333 | 0.097159056 | 3.139587864 | 5.499541705 | 0.007582459 | 5.700389376 | 0.17902593 | 1.35914E-19 | 2.417160847 | 1.692870435 | 1.11132E-07 | 0.94612035 | 0.094026679 | 0.050264597 | 0.947398119 | 1.109215017 | 0.023465625 | 0.039055665 | NaN | -0.072189777 | NaN | NaN | NaN |
| 2 5 | 87.14896194 | 0.191666667 | 0.5483025 | 18.87011398 | 285.7142857 | 0.662133636 | 2.371827833 | 0.333284552 | 0 | 5.791307611 | 53.79931269 | 0.000112 | 4.251868485 | 0.379022531 | 0 | 1.819361063 | 3.645897174 | 0.010500105 | 0.014182297 | 1.888138414 | 0.415729553 | 0.123539113 | 0.354799621 | 0.065258536 |
| 3 5 | -25.60401344 | 0.183333333 | 0.194943823 | 7.482463992 | 14.78560867 | 0.045526704 | 2.087895876 | 0.232658033 | 1.48826E-72 | 5.67776301 | 18.37416202 | 1.11022E-16 | 4.765203544 | 0.560271372 | 0 | 1.53468781 | 1.694171956 | 0.021631255 | 0.023465404 | 1.968933028 | 0.167668641 | 0.113525584 | 0.352727363 | 0.035244249 |
| 3 7 | 74.39598656 | 0.366666667 | 0.264573488 | 22.55592314 | 173.4104046 | 0.595111928 | 2.623041071 | 0.217453163 | 9.18888-132 | 8.293771928 | 59.07768716 | 1.49046E-06 | 4.450624742 | 0.348560261 | 0 | 2.067827298 | 3.737133808 | 0.010762887 | 0.011673284 | 2.652707289 | 0.410882801 | 0.154759735 | 0.418604288 | 0.034773089 |
| 3 8 | -25.60401344 | 0.283333333 | 0.361963125 | 12.13836678 | 151.5151515 | 0.616531106 | 2.844417697 | 0.106714752 | 1.09056E-08 | 3.55190151 | 10.68905611 | 0.014419146 | 4.80287125 | 0.3196632 | 3.90432E-79 | 1.468817204 | 1.682758621 | 0.019582155 | 0.027763492 | 2.18779909 | 0.141037484 | 0.139117151 | 0.36367121 | 0.031747672 |
| 3 11 | -25.60401344 | 0.575 | -0.19096249 | 0.184767322 | 0.409001612 | 0.031736872 | 1.816963416 | 0.166217826 | 0.245379686 | 0.154847766 | 0.563240661 | 0.007008132 | 2.798512297 | 0.09442027 | 0.453497438 | 1.188405797 | 1.022727273 | 0.099003333 | 0.032744144 | NaN | 0.031249398 | NaN | NaN | NaN |
| 4 2 | NaN | 0.266666667 | 0.45743513 | 6.785950396 | 27.8551532 | 0.069269166 | 5.530717009 | 0.071497156 | 0.000575626 | 6.129939103 | 23.97403685 | 8.70548E-12 | 4.439691769 | 0.185828927 | 4.77594E-14 | 3.069230769 | 2.853582555 | 0.017085546 | 0.023171168 | 2.494117647 | 0.125912026 | 0.106115066 | 0.276558405 | 0.019792517 |
| 4 3 | NaN | 0.25 | 0.402280627 | 30.7620074 | 54.64480874 | 0.237560837 | 0.068434637 | 0.185512896 | 1.7113E-135 | 24.70584109 | 70.61348409 | 1.11022E-16 | 4.559324829 | 0.240974677 | 8.42969E-68 | 1.717687075 | 4.725043783 | 0.011463736 | 0.011939734 | 2.095393839 | 0.220934212 | 0.096979903 | 0.253314081 | 0.086790568 |
| 4 8 | NaN | 0.35 | 0.161179724 | 1.892672008 | 8.844339623 | 0.059565511 | 0.553094164 | 0.114519975 | 0.013302151 | 1.693957823 | 2.983668342 | 0.18742396 | 4.131517249 | 0.360768056 | 4.52153E-07 | 1.21875 | 1.2 | 0.027854386 | 0.041036201 | NaN | -0.003285557 | NaN | NaN | NaN |
| 5 4 | -47.54089572 | 0.283333333 | 0.269913118 | 12.67177049 | 88.49557522 | 0.470837092 | 2.121958039 | 0.168875194 | 2.17869E-54 | 5.22962195 | 27.24545744 | 7.85683E-10 | 4.339380487 | 0.301730858 | 0 | 1.474925478 | 2.398322851 | 0.017517841 | 0.025244022 | 1.481502178 | 0.213056612 | 0.130629778 | 0.255303069 | 0.013428863 |
| 6_15 | -71.88211722 | 0.2 | 0.47285508 | 25.67061703 | 66.96428571 | 0.182362214 | 5.595005329 | 0.15065681 | 6.68421E-88 | 24.42501048 | 25.42476978 | 0.912590877 | 5.042183007 | 0.170822366 | 8.55917E-32 | 0.998702525 | 2.355947712 | 0.013713275 | 0.016271619 | NaN | 0.098002173 | NaN | NaN | NaN |
| 7 10 | -551.9782049 | 0.333333333 | -0.284402809 | 11.76207856 | 24.89626556 | 0.089469268 | 5.511597517 | 0.011421037 | 0.735842003 | 8.133870653 | 7.094594595 | 1.85807E-07 | 0.852994522 | 0.074438007 | 0.000544454 | 0.864506307 | 1.455934195 | 0.026514175 | 0.030097726 | NaN | 0.010604889 | NaN | NaN | NaN |
| 7 13 | -351.9782049 | 0.308333333 | 0.412948571 | 16.84425652 | 38.61003861 | 0.087818962 | 2.182225087 | 0.271340683 | 3.31E-213 | 10.72748316 | 41.68002748 | 8.73897E-19 | 4.770534327 | 0.407065586 | 0 | 1.668092618 | 2.822411788 | 0.016604248 | 0.015993669 | 1.426153324 | 0.148290366 | 0.037282396 | 0.236518416 | 0.035979842 |
| 7 14 | -101.9782049 | 0.25 | 0.11187315 | 25.75198226 | 64.65517241 | 0.288546585 | 2.196315462 | 0.268971774 | 0 | 14.72120805 | 61.97320202 | 3.33067E-16 | 4.274165149 | 0.074767825 | 2.44969E-30 | 1.755015045 | 3.876432665 | 0.012193787 | 0.01173142 | 1.262343843 | 0.175469041 | 0.083123162 | 0.204813082 | 0.021169673 |
| 7 15 | -201.9782049 | 0.233333333 | 0.517718026 | 21.37774802 | 122.9508197 | 0.539949968 | 2.06146421 | 0.23372045 | 9.1627E-138 | 8.636959690 | 36.33188273 | 3.2885E-06 | 4.990513745 | 0.077567129 | 8.38338E-19 | 1.715941614 | 2.775590551 | 0.015338548 | 0.018252615 | 1.620601936 | 0.143852532 | 0.045360063 | 0.236350603 | 0.025583957 |
| 8 4 | NaN | 0.316666667 | 0.097058994 | 8.724201607 | 18.35985312 | 0.113817807 | 0.259837805 | 0.261175231 | 2.8813E-110 | 7.05431549 | 12.14931443 | 0.004279917 | 5.054302391 | 0.244629157 | 9.47644E-14 | 1.236137667 | 1.544642857 | 0.020000654 | 0.030052935 | 1.210409036 | 0.033985615 | 0.048495546 | 0.355788491 | 0.012620691 |
| 8 12 | NaN | 0.391666667 | -0.232147968 | 9.506987777 | 18.4729064 | 0.018302346 | 5.69046259 | 0.237489155 | 1.25364E-64 | 7.982565514 | 2.240005869 | 0.07613908 | 4.376582795 | 0.149586267 | 0.00080717 | 0.956066946 | 1.523809524 | 0.020652782 | 0.0260648 | NaN | -0.025096403 | NaN | NaN | NaN |
| 9 17 | NaN | 0.308333333 | -0.337506428 | 32.47436212 | 132.7433628 | 0.545012485 | 6.204750192 | 0.3312694 | 1.4548E-279 | 18.95076083 | 25.42208175 | 0.000110828 | 5.063976554 | 0.201932258 | 9.07138E-44 | 1.111791106 | 3.007592191 | 0.012446535 | 0.025435648 | 1.388756645 | 0.078825124 | 0.085663691 | 0.166688966 | 0.02944254 |
| 10 9 | -41.8014161 | 0.216666667 | -0.250867822 | 10.05181969 | 31.38075314 | 0.147509415 | 0.967135751 | 0.111970864 | 0.035915225 | 6.101757224 | 17.35584334 | 1.27428E-07 | 6.014774394 | 0.089167882 | 3.29359E-05 | 1.309667674 | 1.795103448 | 0.022279644 | 0.028759075 | 1.560493827 | 0.104946285 | 0.092990942 | 0.172336079 | 0.014462396 |
| 11 17 | NaN | 0.283333333 | 0.220256024 | 10.25190572 | 63.69426752 | 0.30537331 | 3.896149212 | 0.128238937 | 0.013771222 | 5.4154702 | 13.80965923 | 1.56956E-08 | 2.147817503 | 0.022673194 | 0.421898163 | 1.357889605 | 2.156766706 | 0.020924105 | 0.029661765 | NaN | 0.067516617 | NaN | NaN | NaN |
| 12 1 | 15.26160312 | 0.175 | 0.754407868 | 22.66992898 | 55.86592179 | 0.219504068 | 1.203989269 | 0.282461922 | 0 | 17.52374621 | 64.87982846 | 6.27797E-18 | 4.612985995 | 0.295802547 | 0 | 1.597203617 | 4.600922442 | 0.012043253 | 0.012838795 | 1.321709429 | 0.345898181 | 0.092692643 | 0.093398023 | 0.033465091 |
| 12 12 | -84.73839688 | 0.191666667 | -0.005400842 | 27.9957558 | 62.5 | 0.209951188 | 0.465572816 | 0.293772017 | 0 | 24.94192369 | 20.19803349 | 0.000863102 | 6.050706444 | 0.091953567 | 6.53071E-39 | 0.889472961 | 2.541675641 | 0.016633142 | 0.022450952 | 1.267535029 | -0.004776817 | 0.048264746 | 0.24254947 | 0.047335233 |
| 12 13 | -184.7383969 | 0.291666667 | 0.204065391 | 6.740315812 | 90.36144579 | 0.501687791 | 3.322814744 | 0.247043456 | 7.86302E-40 | 3.895313103 | 3.871532223 | 0.001174345 | 4.944550338 | 0.147469659 | 6.9273E-20 | 1.365449628 | 1.649990591 | 0.020923644 | 0.036847100 | NaN | 0.02993116 | NaN | NaN | NaN |
| 13 6 | NaN | 0.333333333 | -0.078376253 | 10.56569744 | 31.41361257 | 0.109425664 | 1.478432739 | 0.36787162 | 2.0957E-284 | 9.600664784 | 17.87071108 | 3.76704E-11 | 4.509919637 | 0.020479139 | 0.274119829 | 1.1015625 | 1.929896907 | 0.025316334 | 0.027426009 | 1.164215686 | 0.143046001 | 0.047330223 | 0.216500806 | 0.023708522 |
| 13 17 | 70.45359405 | 0.341666667 | 0.313840844 | 4.038347828 | 7.473841555 | 0.014487276 | 2.093411833 | 0.286920207 | 1.59260E-55 | 3.551128273 | 9.34566949 | 3.76987E-08 | 2.96529369 | 0.209122162 | 1.99965E-19 | 1.150071124 | 1.42503639 | 0.034405594 | 0.031246737 | 1.224770642 | 0.056501895 | 0.040423527 | 0.224482104 | 0.017259399 |
| 13_18 | 24.72272165 | 0.591666667 | 0.017083734 | 4.131766586 | 8.685581954 | 0.022241372 | 1.554138637 | 0.387757236 | 1.0554E-99 | 3.791018286 | 5.765867591 | 5.22084E-07 | 0.923143583 | 0.188803127 | 4.63687E-10 | 1.070080863 | 1.330596476 | 0.057190444 | 0.037554982 | NaN | 0.073163837 | NaN | NaN | NaN |
| 13 37 | -25.27727855 | 0.258333333 | 0.28080317 | 16.72122681 | 41.15226337 | 0.118874525 | 1.847959018 | 0.272054347 | 3.5058E-195 | 14.63611796 | 54.03114352 | 2.55668E-17 | 3.467494796 | 0.178761119 | 5.70965E-79 | 1.387262984 | 4.063179008 | 0.011473572 | 0.014059636 | 1.008474576 | 0.347668764 | 0.012776277 | 0.258548994 | 0.144067991 |
| 14 8 | -108.6963636 | 0.316666667 | -0.631918275 | 3.354512894 | 5.976095617 | 0.003550175 | 0.112502018 | 0.530538901 | 0 | 3.15136838 | 3.216817368 | 3.17319E-08 | 0.662148956 | 0.523767809 | 4.3562E-169 | 1.047012506 | 1.130212766 | 0.027143137 | 0.031514622 | 0.934136771 | -0.050732978 | 0.045819838 | 0.190605287 | 0.004427417 |
| 14 13 | -208.6963636 | 0.225 | 0.619235267 | 3.20666587 | 6.570302234 | 0.04857609 | 1.459317861 | 0.354049433 | 0 | 2.976799322 | 5.195838291 | 5.66214E-15 | 4.211503761 | 0.241863655 | 1.28891E-55 | 1.155615697 | 1.198993851 | 0.024568633 | 0.026395143 | NaN | 0.023570795 | NaN | NaN | NaN |
| 14 22 | -108.6963636 | 0.508333333 | -0.533956963 | 8.751068208 | 15.52795031 | 0.044086658 | 1.656699009 | 0.22614228 | 1.5848E-302 | 3.366991616 | 6.712199489 | 5.24875E-20 | 4.034155874 | 0.143775084 | 2.19355E-25 | 0.908845482 | 1.283464567 | 0.02577756 | 0.029122148 | 1.087061841 | -0.044433825 | 0.082375608 | 0.412173133 | 0.018217142 |
| 15 15 | NaN | 0.183333333 | 0.43901236 | 9.435509971 | 18.10500905 | 0.124466996 | 1.263446075 | 0.244821265 | 0 | 0.780652968 | 15.65872611 | 7.77156E-16 | 5.012117948 | 0.146861517 | 2.11594E-45 | 1.127366609 | 1.6625 | 0.02459972 | 0.024447947 | NaN | 0.055295311 | NaN | NaN | NaN |
| 15 17 | NaN | 0.325 | 0.924707825 | 5.512566823 | 40.10695187 | 0.065669807 | 1.421560619 | 0.338267948 | 1.0282E-224 | 5.279471288 | 2.662114255 | 1.08389E-07 | 4.818658269 | 0.367914591 | 1.1329E-49 | 1.202654867 | 1.423076923 | 0.023028099 | 0.032946154 | NaN | 0.052848615 | NaN | NaN | NaN |
| 18 10 | -10.91994241 | 0.241666667 | 0.563974861 | 16.37899523 | 41.09589041 | 0.165307536 | 2.581436593 | 0.308727958 | 0 | 15.29893879 | 21.9576955 | 2.1023E-09 | 4.569026434 | 0.084177181 | 6.1915E-56 | 1.019718467 | 1.886541943 | 0.018281548 | 0.022322085 | 1.22157558 | 0.00826389 | 0.047097124 | 0.29901424 | 0.031143245 |
| 18 11 | 314.0800576 | 0.583333333 | -0.286067228 | 8.140799773 | 23.16602317 | 0.011341428 | 0.595853835 | 0.508278981 | 0 | 7.882451096 | 2.104923088 | 4.72105E-21 | 3.578711147 | 0.146398913 | 5.51187E-16 | 0.652305825 | 1.280626781 | 0.017571066 | 0.0196077 | 1.131960557 | -0.04614779 | 0.078009695 | 0.055274527 | 0.010835228 |
| 18 13 | 289.0800576 | 0.675 | -0.441062865 | 4.981701355 | 9.140767824 | 0.165817697 | 0.003532983 | 0.108710535 | 4.39527E-40 | 4.79511056 | 1.653129945 | 1.35166E-22 | 3.397078869 | 0.213540558 | 2.20836E-27 | 0.660620188 | 1.254515274 | 0.015473082 | 0.024872535 | 1.239699053 | -0.057832882 | 0.044687286 | 0.199093008 | 0.006379539 |
| 18 23 | 459.0800576 | 0.591666667 | -0.18337031 | 8.388052194 | 24.23263328 | 0.030664533 | 0.593265409 | 0.298510682 | 1.0778E-264 | 8.097668564 | 2.437402539 | 5.12672E-09 | 3.394339604 | 0.054282106 | 0.003159392 | 0.86550497 | 1.735 | 0.014785941 | 0.019443739 | NaN | -0.079460159 | NaN | NaN | NaN |
| 18 29 | 139.0800576 | 0.591666667 | -0.058069902 | 2.524061122 | 5.279366476 | 0.111766639 | 2.117999457 | 0.079193234 | 7.41946E-15 | 2.401342891 | 1.640154158 | 3.58189E-09 | 3.563590356 | 0.388920222 | 1.15421E-92 | 0.824099723 | 1.147420147 | 0.017803148 | 0.028681188 | NaN | -0.044575561 | NaN | NaN | NaN |
| 18 41 | 314.0800576 | 0.583333333 | -0.336534067 | 1.259348447 | 7.211558461 | 0.174958814 | 1.305195038 | 0.1236463 | 9.39301E-14 | 1.20635434 | 0.364088468 | 2.85179E-17 | 3.270716663 | 0.21258738 | 1.18509E-06 | 0.607050731 | 1.358078603 | 0.012975203 | 0.020549353 | NaN | -0.026302518 | NaN | NaN | NaN |
| 19 16 | 225.4251052 | 0.333333333 | 0.283499301 | 6.99447281 | 24.48979592 | 0.03867567 | 1.444067116 | 0.503827358 | 0 | 6.253516369 | 5.314767463 | 5.30676E-09 | 1.119304133 | 0.267847784 | 1.661E-105 | 0.845925824 | 1.316019033 | 0.024772689 | 0.033417519 | 1.565571755 | 0.023147123 | 0.065302297 | 0.361461634 | 0.012220651 |
| 19 22 | 0.425105165 | 0.291666667 | 0.466671554 | 10.07481288 | 23.41920375 | 0.021563515 | 2.308700362 | 0.280383126 | 0 | 9.473672618 | 11.93300607 | 1.04435E-06 | 3.415267702 | 0.213302757 | 2.44196-149 | 0.889102288 | 1.412869283 | 0.022350398 | 0.024248077 | 0.991571326 | -0.017829569 | -0.006377515 | 0.371348104 | 0.019159144 |

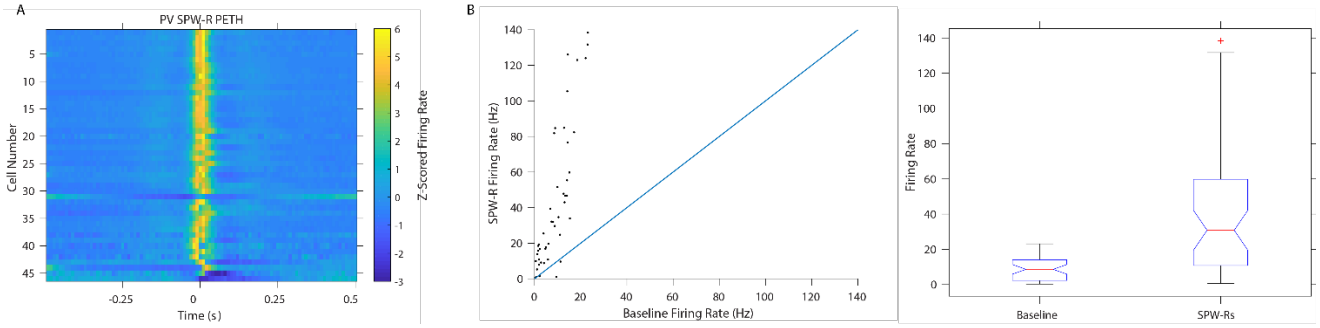


**A.) Figure S1: PV+ cells increase their firing rate during SPW-R.**

B.) Peri-event time histogram of PV z-scored firing rate centered on SPW-R peak (n=46 cells, n=6 animals, 11 sessions. 2031-10,960 SPW-R events, μ= 6,725.6 events)

C.) Left: Firing rate (Hz) in baseline and within SPW-R. (n=46 cells, n=6 animals, 11 sessions. baseline x̃= 8.63Hz, SPW-R x̃= 30.82Hz, p=3.0939e-4, Wilcoxon signed rank test) Right: Distribution of delta firing rate in and out of SPW-R (n=46 cells).

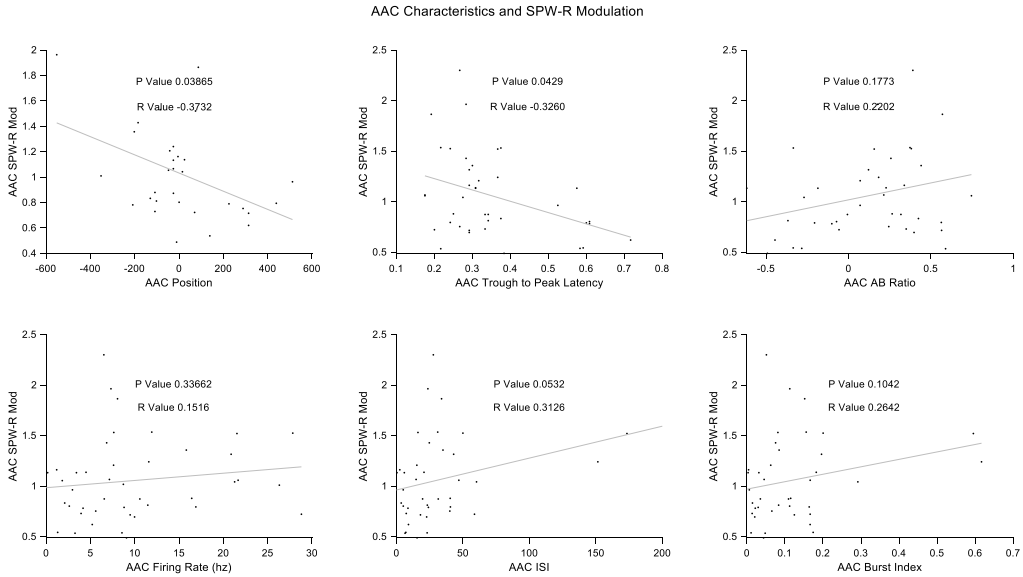


## Figure S2: Spiking activity outside of SPW-R does not explain AAC SPW-R Modulation

Only AAC soma position and trough to peak latency of spikes were significantly correlated to SPW-R modulation.

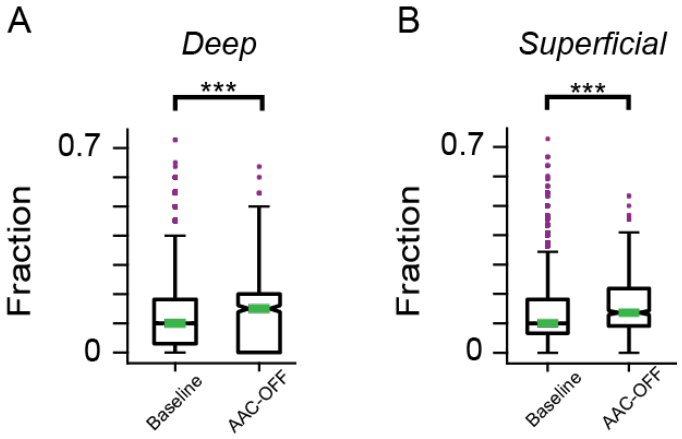


**Figure S3: Both the fraction of deep and superficial PYRs participating is increased in AAC-OFF SPW-R**

. PYR cell participation separated by soma depth (n=1495-12364, total: 37032 Control SPW-R. n=51-287, total: 868 AAC-OFF SPW-R.)

A.) Fraction of Deep PYR participating in SPW-R (n=11-32, total: 125 Deep cells, p= 2.4645e-13, Wilcoxon rank-sum test).

B.) Fraction of Superficial PYR participating in SPW-R (n=5-33, total: 69 Superficial cells. p= 6.5141e-06, Wilcoxon rank-sum test).

## References

1. Bugeon, S. *et al.* A transcriptomic axis predicts state modulation of cortical interneurons. *Nature* **607**, 330–338 (2022).
2. Harris, K. D. *et al.* Classes and continua of hippocampal CA1 inhibitory neurons revealed by single-cell transcriptomics. *PLOS Biology* **16**, e2006387 (2018).

417 3. Klausberger, T. *et al.* Brain-state- and cell-type-specific firing of hippocampal
418 interneurons in vivo. *Nature* **421**, 844–848 (2003).
419 4. Klausberger, T. & Somogyi, P. Neuronal Diversity and Temporal Dynamics:
420 The Unity of Hippocampal Circuit Operations. *Science* **321**, 53–57 (2008).
421 5. Lapray, D. *et al.* Behavior-dependent specialization of identified hippocampal
422 interneurons. *Nat Neurosci* **15**, 1265–1271 (2012).
423 6. Buzsáki, G. & Chrobak, J. J. Temporal structure in spatially organized neuronal
424 ensembles: a role for interneuronal networks. *Current Opinion in Neurobiology*
425 **5**, 504–510 (1995).
426 7. Cobb, S. R., Buhl, E. H., Halasy, K., Paulsen, O. & Somogyi, P.
427 Synchronization of neuronal activity in hippocampus by individual GABAergic
428 interneurons. *Nature* **378**, 75–78 (1995).
429 8. Tremblay, R., Lee, S. & Rudy, B. GABAergic Interneurons in the Neocortex:
430 From Cellular Properties to Circuits. *Neuron* **91**, 260–292 (2016).
431 9. Klausberger, T. *et al.* Spike timing of dendrite-targeting bistratified cells during
432 hippocampal network oscillations in vivo. *Nat Neurosci* **7**, 41–47 (2004).
433 10. Klausberger, T. *et al.* Complementary roles of cholecystokinin- and
434 parvalbumin-expressing GABAergic neurons in hippocampal network
435 oscillations. *J Neurosci* **25**, 9782–9793 (2005).

436 11. Royer, S. *et al.* Control of timing, rate and bursts of hippocampal place cells by
437 dendritic and somatic inhibition. *Nat Neurosci* **15**, 769–775 (2012).
438 12. English, D. F. *et al.* Excitation and inhibition compete to control spiking during
439 hippocampal ripples: intracellular study in behaving mice. *The Journal of*
440 *Neuroscience* **34**, 16509–16517 (2014).
441 13. Dudok, B. *et al.* Alternating sources of perisomatic inhibition during behavior.
442 *Neuron* **109**, 997-1012.e9 (2021).
443 14. Dudok, B. *et al.* Recruitment and inhibitory action of hippocampal axo-axonic
444 cells during behavior. *Neuron* **109**, 3838-3850.e8 (2021).
445 15. Li, X.-G., Somogyi, P., Tepper, J. M. & Buzs□ki, G. Axonal and dendritic
446 arborization of an intracellularly labeled chandelier cell in the CA1 region of rat
447 hippocampus. *Exp Brain Res* **90**, (1992).
448 16. Somogyi, P. A specific 'axo-axonal' interneuron in the visual cortex of the rat.
449 *Brain Res* **136**, 345–350 (1977).
450 17. Varga, C. *et al.* Functional fission of parvalbumin interneuron classes during
451 fast network events. *Elife* **3**, (2014).
452 18. Viney, T. J. *et al.* Network state-dependent inhibition of identified hippocampal
453 CA3 axo-axonic cells in vivo. *Nat Neurosci* **16**, 1802–1811 (2013).

454 19. Geiller, T. *et al.* Large-Scale 3D Two-Photon Imaging of Molecularly
455 Identified CA1 Interneuron Dynamics in Behaving Mice. *Neuron* **108**, 968-
456 983.e9 (2020).
457 20. Vancura, B., Geiller, T., Grosmark, A., Zhao, V. & Losonczy, A. Inhibitory
458 control of sharp-wave ripple duration during learning in hippocampal recurrent
459 networks. *Nat Neurosci* **26**, 788–797 (2023).
460 21. Mizuseki, K., Royer, S., Diba, K. & Buzsáki, G. Activity dynamics and
461 behavioral correlates of CA3 and CA1 hippocampal pyramidal neurons.
462 *Hippocampus* **22**, 1659–1680 (2012).
463 22. Montijn, J. S. *et al.* A parameter-free statistical test for neuronal
464 responsiveness. *eLife* **10**, e71969 (2021).
465 23. Barthó, P. *et al.* Characterization of Neocortical Principal Cells and
466 Interneurons by Network Interactions and Extracellular Features. *Journal of*
467 *Neurophysiology* **92**, 600–608 (2004).
468 24. English, D. F. *et al.* Pyramidal Cell-Interneuron Circuit Architecture and
469 Dynamics in Hippocampal Networks. *Neuron* **96**, 505-520.e7 (2017).
470 25. Stark, E. *et al.* Pyramidal cell-interneuron interactions underlie hippocampal
471 ripple oscillations. *Neuron* **83**, 467–480 (2014).
472 26. Lee, S.-H. *et al.* Parvalbumin-positive basket cells differentiate among
473 hippocampal pyramidal cells. *Neuron* **82**, 1129–1144 (2014).

27. Mizuseki, K., Diba, K., Pastalkova, E. & Buzsáki, G. Hippocampal CA1 pyramidal cells form functionally distinct sublayers. *Nature Neuroscience* **14**, 1174–1181 (2011).
28. Buzsáki, G. Two-stage model of memory trace formation: a role for 'noisy' brain states. *Neuroscience* **31**, 551–570 (1989).
29. Buzsáki, G., Horváth, Z., Urioste, R., Hetke, J. & Wise, K. High-frequency network oscillation in the hippocampus. *Science* **256**, 1025–1027 (1992).
30. Nádasdy, Z., Hirase, H., Czurkó, A., Csicsvari, J. & Buzsáki, G. Replay and time compression of recurring spike sequences in the hippocampus. *The Journal of Neuroscience* **19**, 9497–9507 (1999).
31. O'Neill, J., Senior, T. & Csicsvari, J. Place-Selective Firing of CA1 Pyramidal Cells during Sharp Wave/Ripple Network Patterns in Exploratory Behavior. *Neuron* **49**, 143–155 (2006).
32. Topolnik, L. & Tamboli, S. The role of inhibitory circuits in hippocampal memory processing. *Nat Rev Neurosci* **23**, 476–492 (2022).
33. Andersen, P., Eccles, J. C. & LøYNING, Y. Hippocampus of the Brain: Recurrent Inhibition in the Hippocampus with Identification of the Inhibitory Cell and its Synapses. *Nature* **198**, 540–542 (1963).
34. McKenzie, S. Inhibition shapes the organization of hippocampal representations. *Hippocampus* **28**, 659–671 (2018).

35. Lee, J. S., Briguglio, J. J., Cohen, J. D., Romani, S. & Lee, A. K. The Statistical Structure of the Hippocampal Code for Space as a Function of Time, Context, and Value. *Cell* **183**, 620-635.e22 (2020).
36. Szabo, G. G. *et al.* Ripple-selective GABAergic projection cells in the hippocampus. *Neuron* **110**, 1959-1977.e9 (2022).
37. Petersen, P. C., Hernandez, M. & Buzsáki, G. The Buzsaki Lab Databank - Public electrophysiological datasets from awake animals. Zenodo https://doi.org/10.5281/zenodo.4307883 (2020).
38. Pachitariu, M., Steinmetz, N., Kadir, S., Carandini, M. & Kenneth D., H. *Kilosort: Realtime Spike-Sorting for Extracellular Electrophysiology with Hundreds of Channels*. http://biorxiv.org/lookup/doi/10.1101/061481 (2016) doi:10.1101/061481.
39. Kadir, S. N., Goodman, D. F. M. & Harris, K. D. High-Dimensional Cluster Analysis with the Masked EM Algorithm. *Neural Computation* **26**, 2379–2394 (2014).
40. Petersen, P. C., Siegle, J. H., Steinmetz, N. A., Mahallati, S. & Buzsáki, G. CellExplorer: A framework for visualizing and characterizing single neurons. *Neuron* **109**, 3594-3608.e2 (2021).